Geophys. J. Int. (2009) **176,** 95–106 doi: 10.1111/j.1365-246X.2008.03978.x

Estimating the rates of mass change, ice volume change and snow volume change in Greenland from ICESat and GRACE data

D. C. Slobbe, P. Ditmar and R. C. Lindenbergh

Delft Institute of Earth Observation and Space Systems, Delft University of Technology, Delft, the Netherlands. E-mail: D.C.Slobbe@tudelft.nl

Accepted 2008 September 15. Received 2008 June 20; in original form 2008 February 29

SUMMARY

The focus of this paper is on the quantification of ongoing mass and volume changes over the Greenland ice sheet. For that purpose, we used elevation changes derived from the Ice, Cloud, and land Elevation Satellite (ICESat) laser altimetry mission and monthly variations of the Earth's gravity field as observed by the Gravity Recovery and Climate Experiment (GRACE) mission.

Based on a stand alone processing scheme of ICESat data, the most probable estimate of the mass change rate from 2003 February to 2007 April equals -139 ± 68 Gton yr^{-1}. Here, we used a density of 600 ± 300 kg m^{-3} to convert the estimated elevation change rate in the region above 2000 m into a mass change rate. For the region below 2000 m, we used a density of 900 ± 300 kg m^{-3}.

Based on GRACE gravity models from half 2002 to half 2007 as processed by CNES, CSR, DEOS and GFZ, the estimated mass change rate for the whole of Greenland ranges between -128 and -218 Gton yr^{-1}.

Most GRACE solutions show much stronger mass losses as obtained with ICESat, which might be related to a local undersampling of the mass loss by ICESat and uncertainties in the used snow/ice densities.

To solve the problem of uncertainties in the snow and ice densities, two independent joint inversion concepts are proposed to profit from both GRACE and ICESat observations simultaneously. The first concept, developed to reduce the uncertainty of the mass change rate, estimates this rate in combination with an effective snow/ice density. However, it turns out that the uncertainties are not reduced, which is probably caused by the unrealistic assumption that the effective density is constant in space and time. The second concept is designed to convert GRACE and ICESat data into two totally new products: variations of ice volume and variations of snow volume separately. Such an approach is expected to lead to new insights in ongoing mass change processes over the Greenland ice sheet. Our results show for different GRACE solutions a snow volume change of -11 to 155 km^3 yr^{-1} and an ice loss with a rate of -136 to -292 km^3 yr^{-1}.

Key words: Sea level change; Time variable gravity; Glaciology; Arctic region.

1 INTRODUCTION

The predicted sea level rise in the 21st century as indicated in the Fourth Assessment Report of the Intergovernmental Panel on Climate Change (IPCC 2007) ranges between 18 and 59 cm. These predictions do not yet include the contributions of the dynamic response of the ice sheets to increasing temperatures, due primarily to a limited understanding of the corresponding processes. It is likely that these predictions are too low and, therefore, a detailed knowledge of the evolution of the polar ice sheets is of considerable societal importance.

Monitoring ice mass variations in polar areas is one of the objectives of the Gravity Recovery and Climate Experiment (GRACE) mission and the Ice, Cloud, and land Elevation Satellite (ICESat) mission, launched in 2002 March and 2003 January, respectively. Since then, GRACE data are used to compute time-series of models that reflect temporal variations of the Earth's gravity field. A typical temporal sampling of such a series is 1 month. The computed models can be used to monitor a mass re-distribution at the Earth's surface with a spatial resolution of 300–500 km. The ICESat mission measures, amongst others, elevation changes of the Greenland and Antarctic ice sheets with a nearly complete coverage and high spatial resolution.

The temporal coverage of ICESat is limited, because there are only 2 or 3 measurement campaigns of $\sim$35 d yr^{-1}. In this paper, we use ICESat data to estimate elevation changes in Greenland with

the same temporal resolution as in the case of GRACE: 1 month. Of course, this can be done only for the months covered by the available observation campaigns.

Currently, several estimates of Greenland's ice sheet mass change rates are available, which are obtained from GRACE (Chen *et al.* 2006; Luthcke *et al.* 2006; Ramillien *et al.* 2006; Velicogna & Wahr 2005, 2006, 2007), and ICESat (Thomas *et al.* 2006) data, sometimes in combination with data from other sources. The estimates show a larger spread than could be expected from the reported uncertainties, which indicates that these uncertainties are too optimistic. Furthermore, virtually no attempts were made so far to combine the GRACE and ICESat data sets in a joint inversion scheme. An exception is the research of Wahr *et al.* (2000), who proposed a combination concept aimed at a simultaneous estimation of the mass change rate and postglacial rebound (PGR) over the Antarctic ice sheet. However, that methodology is hardly relevant for Greenland, because the average contribution of PGR is believed to be low (Velicogna & Wahr 2005).

Development of a new joint inversion scheme to combine ICESat and GRACE data over Greenland is the primary subject of this paper. Here, we focus on integrated estimations for the whole of Greenland. Two different concepts of joint inversion are proposed. The first concept aims at the usage of both data sets for estimating simultaneously the mass change rate and effective snow/ice density. We investigate if application of this concept helps to reduce the uncertainty in mass change rates compared to stand alone data processing. The second concept is designed to convert GRACE and ICESat data into two totally new products: variations of ice volume and variations of snow volume separately.

The structure of the paper is as follows. Section 2 starts with a brief introduction of the ICESat data set, followed by a description of the way how the elevation change rates are derived and converted to mass change rates. This section ends with a summary of the results obtained. Section 3 briefly discusses the methodology used to estimate the mass change rate based on GRACE monthly variations of the Earth's gravity field. The section continues with a comparison of the results based on models from different processing centres. In Section 4, we compare our ICESat and GRACE estimates and discuss possible reasons that explain the differences. Section 5 presents the two newly proposed joint inversion concepts and the results obtained on their basis. The last section contains conclusions and recommendations for future work.

2 MASS CHANGE RATE ESTIMATION FROM ICESAT DATA

Several methods to obtain elevation change rates based on ICESat data are developed, for a brief overview we refer to Slobbe *et al.* (2008). We developed our own methodology, which is briefly discussed in the next section.

2.1 Methodology/observation equations

To estimate the mass change rate with ICESat data, the elevation differences of 925 557 geometrically overlapping footprint pairs (see Fig. 1) are retrieved from the level-2 altimetry product (GLA12) that provides the surface elevations for the Greenland and Antarctic ice sheets (Zwally *et al.* 2007). We used the most recent laser campaign releases available at the time of this study, that is, release 228 for laser campaign L1a and the fully calibrated (release 428) laser campaigns L2a to L3h, spanning from 2003 February to 2007 April (five spring, two summer and four fall campaigns). The data are edited using quality flags defined by the GLAS science team, as well as other additional criteria. The obtained elevation differences are corrected, to eliminate biases in the elevation differences caused by not completely overlapping footprint pairs. To this end, we used a digital elevation model generated from the first seven laser campaigns (from 2003 February through 2005 June) of the ICESat mission (DiMarzio *et al.* 2007), to correct for the influence of a non-zero surface slope. The corrected elevation differences $\underline{\Delta H}_{ij}$ are exploited to estimate a time-series of average elevations using the general observation eq. (1).

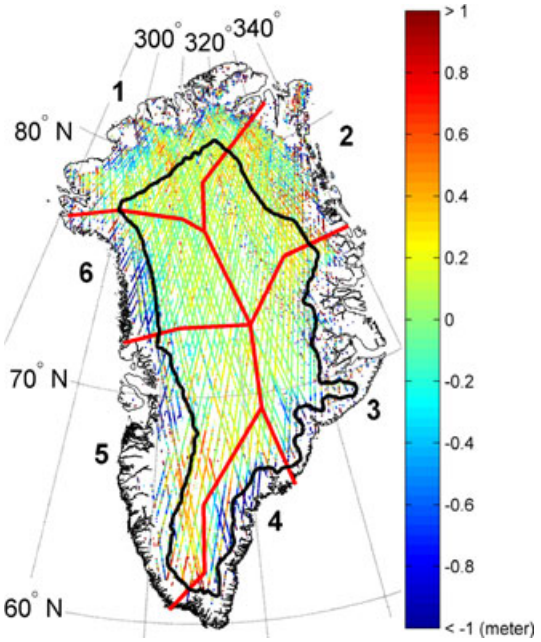

Figure 1. Overview of all elevation differences. The thick black line is the 2000 m elevation contour. The thick red line represents the boundaries of the six drainage systems, which are indicated by the numbers.

$$\underline{\Delta H}_{ij} = H_j^{\mathrm{r}} - H_i^{\mathrm{r}} + \underline{e}_{\Delta H}, \text{ with } i < j, \tag{1}$$

where H_j^{r} and H_i^{r} are the relative heights in month i and j, and $\underline{e}_{\Delta H}$ is the observation error. Note that based on elevation differences only, no absolute height can be estimated. Hence one has to fix the height of one reference epoch (r).

The time-series are used to estimate a linear trend, jointly with the parameters of a seasonal cycle, see eq. (2).

$$H_i = a + \dot{H} t_i + c \sin\left(\frac{2\pi t_i}{T}\right) + d \cos\left(\frac{2\pi t_i}{T}\right) + \underline{e}_H, \tag{2}$$

where a is the y-intercept, $\dot{H}$ the elevation change rate, c and d the parameters that account for the seasonal cycle, T the period of the seasonal cycle, that is, 1 yr and $\underline{e}_H$ is the error in the height.

For more details about the used procedures, we refer to Slobbe *et al.* (2008).

2.2 Division of the ice sheet

From Figs 1 and 3, it follows that most of the overlapping footprint pairs are located in the northern part of the ice sheet, which is a consequence of the convergence of satellite ground tracks towards the poles. When we apply eqs (1) and (2) for Greenland as a whole, the parameter estimates will be biased by a relatively high

contribution of the northern elevation changes. To prevent such an inhomogeneous weighting of the signals, we divided the ice sheet in six drainage systems (taken from Luthcke *et al.* 2006), further divided into a region above and below 2000 m, see Fig. 1. This division will be referred to as division I.

However, for GRACE we only estimate the mass change rate over the whole Greenland ice sheet, which is a consequence of the limited spatial resolution of GRACE. Usage of ICESat and GRACE data in a joint inversion implies that for ICESat we have to join all drainage systems to estimate the changes for the whole of Greenland as well. For both joint inversion schemes (Section 5), the total volume changes between each particular pair of epochs i and j is needed. These quantities are computed as follows. In the first step, the observed elevation differences ($\underline{\Delta H}_{ij}$, eq. 1) are multiplied with the area of the drainage system the overlapping footprint pair belongs to, to obtain multiple estimations of the volume difference ΔV_{ij}. In the second step, the average volume change for each particular pair of epochs ($\overline{\Delta V}_{ij}$) is computed per drainage system. After that, the total volume change over the whole Greenland ice sheet ($\sum \overline{\Delta V}_{ij}$) for each particular pair of epochs is obtained by summation of the averages ($\overline{\Delta V}_{ij}$) per drainage system. For the second joint inversion scheme also, the total volume change rates can be used. To obtain these rates, the total volume changes are used to estimate a time-series using eq. (1), but with $\underline{\Delta H}_{ij}$ replaced by $\sum \overline{\Delta V}_{ij}$ and H^{r}_j and H^{r}_i by the relative volumes V^{r}_j and V^{r}_i, respectively. Again, eq. (2) is used to estimate the volume change rate over the whole Greenland ice sheet, jointly with the parameters of a seasonal cycle.

Unfortunately, not for all drainage system regions, the same pairs of epochs are available. When for a certain region a particular combination of epochs is missing, the sum over the other regions of the average volume changes for that epoch pair is no longer a sum over the whole Greenland ice sheet. For ICESat, we have data for 23 different months, resulting in 253 unique epoch pairs. For none of the drainage system regions, all pairs are available, the maximum is 251, while the minimum is only 110. To solve this problem, we decided to merge drainage system 1, 2 and 6 and drainage system 3, 4 and 5 (see Fig. 1) for the region above and below 2000 m separately. This results in a division into four large regions, referred to as division II. With this approach, we still missed data for 27 epoch pairs for the southern coastal region. So we removed these epoch pairs from the data set.

2.3 Conversion to mass change rates

To convert the estimated volume change rates into mass change rates, different approaches exist (Wingham *et al.* 2006). The main problem is that a proper snow/ice density value is needed. The density of newly fallen snow is about three times smaller than the density of ice (300 kg m^{-3} vs. 900 kg m^{-3};Wingham *et al.* 2006). The proper choice of density depends on whether the changes in elevation of the snow/ice column are caused by ice dynamics, not being in balance with the long-term multidecadal accumulation rate, or are caused by shorter-term (decadal) variability in accumulation (Zwally *et al.* 2005). In the last case, the snow density should be used to convert a volume change to a mass change. In other words, when the mass changes are caused by a change in accumulation, another density has to be used as when they are caused by a change in ablation.

Zwally *et al.* (2005) used an average density of 900 kg m^{-3} based on two assumptions: (i) when the time-series are sufficiently long, short-term stochastic fluctuations in accumulation rate average out over the full period and (ii) over large regions their nett effect will also average out.

In Thomas *et al.* (2006) similar assumptions are made, but different densities are used for different regions. For the region above 2000 m, they used a density of 600 $\pm$ 300 kg m^{-3}, but as they stated, the actual density is probably on the lower side of the indicated range (300–900 kg m^{-3}). This density is chosen because they conclude that the observed elevation differences are mainly caused by increased snowfall. In the region below 2000 m, where mass is lost by ice melting and increased ice discharge, Thomas *et al.* (2006) used a density of 900 kg m^{-3}.

The approach of Thomas *et al.* (2006) is confirmed by recent observations that show that the volume variations below 2000 m are mainly caused by variations in the amount of ice, which are triggered by fluctuations in flow velocity of the glaciers (Howat *et al.* 2007) and (Rignot & Kanagaratnam 2006). For the region above 2000 m, a positive elevation change rate is reported by Johannessen *et al.* (2005), Thomas *et al.* (2006) and Zwally *et al.* (2005). Therefore, we adopted the approach of Thomas *et al.* (2006). Here, we use for all regions above 2000 m a density of 600 ± 300 kg m^{-3}, whereas for the regions below 2000 m a density of 900 ± 300 kg m^{-3} is used. Here, the range of ± 300 kg m^{-3} is used to compute an empirical error. At first glance, $900 + 300$ kg m^{-3} might look strange, but notice that it is an effective density, which can be larger as an actual density. This will be further discussed in Section 5.

The relative large uncertainty in the used densities also reflects the uncertainty introduced by density fluctuations in the snow column, driven by changes in the temperature and accumulation rate (Arthern & Wingham 1998). Such changes influence the rate at which the snow compacts, resulting in elevation changes that will be observed by the satellite altimeters, which are unrelated to mass changes. Based on a firn compaction model, Li *et al.* (2007b) estimated the average signal caused by firn compaction over the whole Greenland ice sheet over a period of 2003–2006 as -5 cm yr^{-1}.

To retrieve the mass change rate for the whole of Greenland, we simply sum up all estimated mass change rates for all different drainage systems both for the regions above and below 2000 m elevation.

2.4 Results and discussion

Using the reported effective densities for the region above and below 2000 m, we estimated the ranges of mass change rates for both ice sheet divisions, as provided in Table 1. For division I, it turns out that the used densities have the largest influence on the estimates for the regions below 2000 m, because here the largest signals are observed. In total, the obtained mass change rate over the whole of Greenland equals -139 ± 68 Gton yr^{-1}. For a further validation of these results, we refer to Slobbe *et al.* (2008).

From Table 1, it follows that the total mass change rate over the whole of Greenland based on division I differs by 10 Gton yr^{-1} from the rate based on division II. This difference is mostly caused by different estimates for the northern coastal region, -25 ± 10 and -16 ± 5 Gton yr^{-1} for divisions I and II, respectively. An additional study showed that the lower estimation for division II is caused by an inhomogeneous distribution of overlapping footprint pairs. Accumulation signals in the northern part of each region are better sampled, which apparantly leads to an underestimation of the observed negative trend when averaging over larger areas is applied, as takes place for division II.

Table 1. Estimated mass change rates in Gton yr^{-1} based on ICESat data (2003 February to 2007 April) for two different divisions (I and II) of the Greenland ice sheet, and for both the region above (↑) and below (↓) 2000 m.

		North				South				Total
Division		1	2	6	1 + 2 + 6	3	4	5	3 + 4 + 5	
I	↑	3 ± 2	7 ± 3	2 ± 1	12 ± 6	0 ± 0	-10 ± 5	10 ± 5	0 ± 10	12 ± 16
	↓	-3 ± 1	3 ± 1	-25 ± 8	-25 ± 10	-30 ± 10	-57 ± 19	-39 ± 13	-127 ± 42	-151 ± 52
	Total	0 ± 3	10 ± 4	-23 ± 9	-13 ± 16	-30 ± 10	-67 ± 24	-29 ± 18	-127 ± 52	-139 ± 68
II	↑				13 ± 6				0 ± 0	13 ± 6
	↓				-16 ± 5				-126 ± 42	-142 ± 47
	Total				-3 ± 11				-126 ± 42	-129 ± 53

Note: For the region above 2000 m, a density of 600 ± 300 kg m^{-3} is used, while for the region below 2000 m, the density is 900 ± 300 kg m^{-3}. Here, the reported empirical error only represents the uncertainty introduced by the used density.

Table 2. Main properties of the used GRACE monthly solutions.

Solution	Release	Time span	Subtracted static field
CNES	1	Aug 2002–Jun 2007	EIGEN-GL04C
CSR	4	Apr 200–Jun 2007	mean 2003–2004
DEOS	1	Feb 2003–Dec 2006	EIGEN-GL04C
GFZ	4	Aug 2002–Jun 2007	EIGEN-GL04C

3 MASS CHANGE RATE ESTIMATION FROM GRACE DATA

To estimate the mass change rate using GRACE observations, monthly models of the Earth's gravity field derived from GRACE observations are used. Different GRACE solutions independently computed by several research groups are available. Here, we used the solutions of the Bureau Gravimetrique International of the Centre National d'Ètudes Spatiales (CNES; Lemoine *et al.* 2007), Center for Space Research (CSR; Bettadpur 2007), GeoForschungsZentrum (GFZ; Schmidt 2007) and Delft Institute of Earth Observation and Space Systems (DEOS; Liu *et al.* 2007). The used GRACE solutions are referred to by the processing centre. Each solution consists of a set of Stokes coefficients C_{lm}. It is important to mention that we restored the secular trends in the low-degree coefficients (c_{20}, c_{21}, s_{21}, c_{30} and c_{40}) that were subtracted to produce the original GRACE models but not restored. The main properties of the used solutions are summarized in Table 2. The monthly gravity variations are obtained by subtracting a mean field from the monthly solutions. Currently we do not consider the degree 1 coefficients, which are not available in the original models, even though they may have some impact on the estimated mass change rate.

3.1 Methodology

A methodology that can be used to derive mass change rates from GRACE data is extensively described (e.g. Wahr *et al.* 1998). Here, we applied almost the same methodology as described in Velicogna & Wahr (2005). Basically, the integrated mass variation $\bar{f}_0$ inside the region Ω_{reg} is given by

$$\bar{f}_0 = \int_{\Omega_{\text{reg}}} f(\theta, \lambda) \mathrm{d}\Omega_R \tag{3}$$

$$= \int_{\Omega_R} f(\theta, \lambda) q(\theta, \lambda) \mathrm{d}\Omega_R, \tag{4}$$

where $f(\theta, \lambda)$ the global mass variation as a function of location, $q(\theta, \lambda)$ is a region function (i.e. 1 inside and 0 outside the area of interest, respectively) and Ω_R the mean Earth sphere.

To reduce the influence of noise, a low-pass Gaussian filter (Wahr *et al.* 1998) with a half-width of 400 km is applied. The mass changes are corrected for the PGR effect by using the PGR-induced rates, calculated using Peltier's ICE-5G ice model and the VM2 Earth model (Peltier 2004). Over the whole of Greenland, the PGR contribution is equal to -4 Gton yr^{-1}. To estimate the uncertainty of this value, we used half the value of the maximum difference among the PGR rates based on different earth models (Riva, personal communication 2008). For Greenland, this results in an uncertainty of 3.2 Gton yr^{-1}.

The main difference between our approach and the approach described in Velicogna & Wahr (2005) is related to the so-called 'leakage effect'. Application of the Gaussian filter for the purpose of noise reduction is known to introduce a bias in the estimated average over the region of interest (Klees *et al.* 2007). This bias $\bar{\epsilon}_0$ can be written as

$$\bar{\epsilon}_0 = -\int_{\Omega_{\text{reg}}} f_0(\theta, \lambda)[1 - q_w(\theta, \lambda)] \mathrm{d}\Omega_R + \int_{\Omega_R - \Omega_{\text{reg}}} f_l(\theta, \lambda) q_w(\theta, \lambda) \mathrm{d}\Omega_R, \tag{5}$$

where $f_0(\theta, \lambda)$ and $f_l(\theta, \lambda)$ are the mass variations inside and outside the region of interest, respectively, and $q_w(\theta, \lambda)$ is the smoothed region function, which is a spherical convolution of the Gaussian filter with the region function $q(\theta, \lambda)$.

The first term on the right-hand side of eq. (5) (the so-called type 1 error) expresses the contribution of mass variations inside the region of interest. The second term (the so-called type 2 error) represents the contribution of mass variations outside the region of interest. In literature, this bias is also called the leakage error.

For Greenland, the type 2 error is caused by contributions from the ocean and the hydrology in surrounding continental areas. In Ramillien *et al.* (2006), the contribution of the type 2 error to the mass change rate was estimated on the basis of the Water Gap Hydrology Model. The obtained value of 1 km^3 yr^{-1} is much smaller than the formal error in the estimated trend. In Velicogna & Wahr (2005), monthly global water storage fields from the Noah Land Surface Model produced with the Global Land Data Assimilation System (GLDAS) were used to estimate the contamination from continental hydrology outside Greenland. Furthermore, they estimated the contamination from the ocean using a JPL version of the ECCO general circulation model. They conclude that the amplitude of leakage is approximately equal to the GRACE error bars. On the basis of these results, we conclude that the type 2 error is negligible in the context of our study.

The type 1 error leads to an underestimation of the mass change since the difference $1 - q_w(\theta, \lambda)$ is always positive. To correct for

the type 1 error, the following procedure is described in Velicogna & Wahr (2005, 2006). The averaging function is scaled so that if it is applied to a uniform mass change of 1 cm water thickness in the coastal area of a few hundred kilometres width, but zero in the interior, it returns an average value of 1 cm for the coastal area. This will result in a scaling factor of 1.95 (Wahr *et al.* 2007). Alternatively, a homogeneous mass change over the whole Greenland ice sheet can be assumed, which results in a scaling factor of 1.85 (Wahr *et al.* 2007). We implemented a similar procedure with this difference that the scaling factor is obtained based on the ICESat estimates per drainage system region, resulting in a scaling factor of 2.05. We believe that this scaling factor is more adequate than the ones obtained in Wahr *et al.* (2007). If the mass changes were located at the coast, and the Greenland continent was a half-plane, exactly one half of the visible mass change after smoothing would be located in-land, that is, the scaling factor would be exactly 2. Since in practice Greenland is not a half-plane and even more than one half of the mass change signal is located off-shore after smoothing, a scaling factor above 2 could be expected. This procedure of leakage correction is referred to as LC1.

The second procedure we implemented to correct for the type 1 error, is based on an enlarging of the region function, that is, the Greenland basin is extended with a buffer. A similar procedure is used by Velicogna & Wahr (2005), however, instead of a Gaussian filter, they used an optimized averaging kernel. If there would be no signal outside Greenland, the size of the buffer could be chosen sufficiently large to ensure that no signal would be lost. Since in practice there are signals outside Greenland, coming from the oceans and surrounding continental areas, a reasonable buffer size has to be chosen, which should be not too large to avoid a contamination from signals outside Greenland. On the other hand, it should not be too small to avoid a signal loss from Greenland. Therefore, we decided to evaluate different buffer sizes ranging from 300 to 1000 km, to derive a reasonable value. The minimum and maximum values of the buffer size are determined by the characteristic half-width of the Gaussian filter used (400 km). Instead of computing the monthly integrated value over the actual Greenland region, the integrated value is computed over the enlarged region. This procedure of leakage correction is referred to as LC2. In the next section, the results obtained with both procedures will be evaluated.

To derive the formal errors of the estimated mass change rates, we need to know the variance of the estimated monthly mass variations. These are obtained by the application of the propagation law of variances on the calibrated standard deviations of the spherical harmonic coefficients available for all GRACE solutions. To obtain the formal error of the estimated mass change rate, we apply eq. (6).

$$\boldsymbol{Q}_{\hat{x}\hat{x}} = (\boldsymbol{A}^T \boldsymbol{Q}_{yy}^{-1} \boldsymbol{A})^{-1}, \tag{6}$$

where $\boldsymbol{Q}_{\hat{x}\hat{x}}$ is the variance–covariance matrix of the unknown parameters, $\boldsymbol{A}$ the design matrix defined by eq. (2) and $\boldsymbol{Q}_{yy}$ the variance–covariance matrix of the obtained monthly masses.

3.2 Results and discussion

With the methodology described in Section 3.1, we derived the mass change rates for the entire Greenland from GRACE data alone, using the procedures (LC1 and LC2) to correct for the leakage effect.

To derive a reasonable value of the buffer size in the second procedure, the estimated mass change rates are plotted as a function of the buffer size (Fig. 2). From this plot, it follows that the estimated mass change rates are converging for the CNES, DEOS and GFZ models, while this convergence is absent for CSR. A convergence can be interpreted as an evidence of the absence of large signals outside Greenland, which justifies this approach (LC2) to correct for signal leakage. An additional study showed that the absence of convergence for the CSR models is partly caused by stripes (Swenson & Wahr 2006), which makes the estimates based on these models less reliable. On the basis of this plot, we chose a buffer size of 600 km as the convergence point, which is a reasonable distance

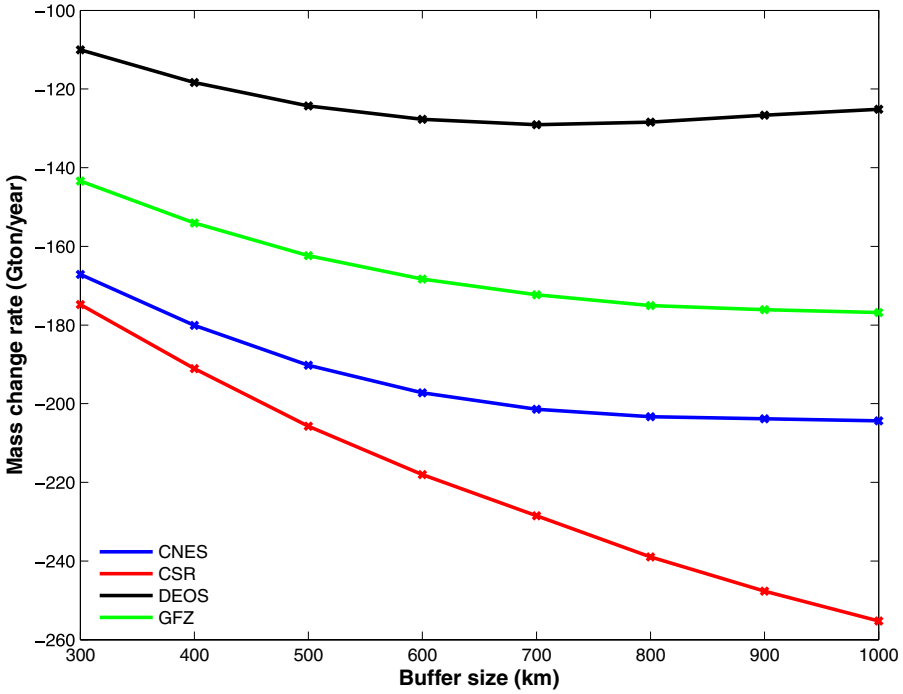

Figure 2. The estimated mass change rate as a function of the buffer size.

Table 3. Estimated mass change rates in Gton yr^{-1} for all used GRACE solutions, using a Gaussian filter with a half-width of 400 km. Two different procedures to account for the leakage effect are used.

	Buffer size	$\dot{M}_{\mathrm{CNES}}$	$\dot{M}_{\mathrm{CSR}}$	$\dot{M}_{\mathrm{DEOS}}$	$\dot{M}_{\mathrm{GFZ}}$
Time span		Aug 2002–Jun 2007	Apr 2002–Jun 2007	Feb 2003–Dec 2006	Aug 2002–Jun 2007
LC1		-202 ± 1	-201 ± 12	-123 ± 1	-172 ± 4
LC2	300	-167 ± 1	-175 ± 12	-110 ± 1	-143 ± 3
LC2	400	-180 ± 1	-191 ± 14	-118 ± 1	-154 ± 4
LC2	500	-190 ± 1	-206 ± 16	-124 ± 1	-162 ± 4
LC2	600	-197 ± 2	-218 ± 18	-128 ± 1	-168 ± 5
LC2	700	-201 ± 2	-228 ± 21	-129 ± 2	-172 ± 6
LC2	800	-203 ± 2	-239 ± 24	-128 ± 2	-175 ± 6
LC2	900	-204 ± 2	-248 ± 26	-127 ± 2	-176 ± 7
LC2	1000	-204 ± 2	-255 ± 29	-125 ± 2	-177 ± 7
Velicogna & Wahr (2007)[a]			-206		-179

Note: LC1 refers to the procedure where the ICESat estimated mass change rates are exploited to compute a scaling factor applied to rescale our estimates accordingly. LC2 refers to the procedure where the mass variations are estimated over an enlarged region. The buffer size refers to the distance used to enlarge the Greenland basin. For comparison reasons, we added in the last row the estimates obtained by Velicogna & Wahr (2007).
[a]No uncertainty measures available.

if we consider the characteristic half-width of the Gaussian filter used (400 km).

The estimated mass change rates and accompanying formal errors are provided in Table 3. Differences in the estimated rates between leakage correction method LC1 and LC2 (using a buffer size of 600 km) depend on the used GRACE solution. For CSR, the difference equals 17 Gton yr^{-1}, but this difference might be partly caused by a contamination of stripes in the buffer region. For CNES and GFZ, the differences are -5 and -4 Gton yr^{-1}, while for DEOS a difference of 5 Gton yr^{-1} is observed. It is worth noticing that only one scaling factor is computed for LC1 solutions. In Wahr *et al.* (2007) it was, however, shown that the scaling factor depends on the spatial distribution of the signal. Since the spatial distribution of the signal dramatically changes over time by seasonal fluctuations and trends that differ over different regions of the ice sheet, the scaling factor must also be time-dependent, which is not taken into account in procedure LC1. Furthermore, there are reasons that may cause an underestimation of the mass loss obtained with ICESat (Section 4). Hence, the scaling factor might be underestimated as well. In future research, a more accurate scale factor might be obtained with the help of simulations with known geographical distribution of major ice dynamic changes (Chen *et al.* 2006). For this reason, we regard the LC2-based values, obtained using a buffer size of 600 km, as our best estimates.

Differences between the different GRACE solutions are rather large (much larger than the formal errors). The largest negative trends (-197 and -218 Gton yr^{-1}) are shown by CNES and CSR solutions, respectively, whereas the smallest negative trend (around -128 Gton yr^{-1}) is demonstrated by the DEOS solution. One may notice that the time interval covered by the DEOS solutions is slightly shorter. An additional analysis has shown, however, that this cannot explain the observed differences. An adequate truncation of the time-series of the other processing centres results in only minor changes in the estimated trends (not more than 10 Gton yr^{-1}). Therefore, the observed differences between GRACE solutions should probably be explained by different data processing strategies and orbits used by the processing centres to obtain the monthly gravity fields.

Importantly, our estimations do not differ significantly from GRACE estimates provided by Velicogna & Wahr (2007) (Table 3) that use data of the same processing centres and a comparable time span. For CSR, differences might be caused by a contamination of the solutions with stripes. Also, the differences might be caused by the different methodologies applied to correct for signal leakage.

4 A COMPARISON OF ICESAT AND GRACE

A comparison of negative trends obtained from ICESat and GRACE (Tables 1 and 3, respectively) shows that the former estimates are somewhat lower. One may argue that this difference might be caused by the fact that only a limited number of months were covered by ICESat observations. To compare the GRACE-based estimates with those based on ICESat data more adequately, we re-processed the series of GRACE models using exactly the same epochs and the same time span as we have for ICESat data, see Table 4. In this way, we exclude temporal differences that might bias the comparison. It is worth mentioning that for DEOS solutions we could not reach perfect matching because they are not yet available for spring 2007.

When we compare different estimates of Greenland's ice sheet mass change rate, we immediately observe the best agreement of the number based on the GRACE DEOS model with the number derived from ICESat data. It is tempting to say that such a consistency is a proof that these numbers are correct. However, it cannot be excluded that this coincidence happened just by chance, and that both of these numbers somewhat underestimate the actual rate. The reason to suspect that the rate derived from ICESat data underestimates the actual trend is based on the fact that ICESat may not give a representative description of a fast ablation in the coastal areas. The ablation pattern is very inhomogeneous over the Greenland ice sheet, that is, strong mass losses can be related to particular glaciers. To obtain a representative estimation of the total mass change rate, all these spots need to be sampled sufficiently and homogeneously, both in the spatial and temporal domains. For ICESat, the sampling mainly depends on the orbital configuration of the satellite and, therefore, becomes less dense for lower latitudes. Furthermore, the sampling is hampered by bad weather conditions, causing large gaps in the observed elevations along track. The sampling heterogeneity is clearly visible from Fig. 3 that shows the number of overlapping footprint pairs as a function of location. It can be seen that along the

Table 4. Estimated mass change rates in Gton yr^{-1} for all used GRACE solutions using (i) all months available, using (ii) only the months for which also ICESat data is available and using (iii) all months available over the same time span as we have data for ICESat (2003 February to 2007 April).

	$\dot{M}_{\mathrm{CNES}}$	$\dot{M}_{\mathrm{CSR}}$	$\dot{M}^{a}_{\mathrm{DEOS}}$	$\dot{M}_{\mathrm{GFZ}}$	$\dot{M}_{\mathrm{ICESat}}$
LC2 600	-197 ± 2	-218 ± 18	-128 ± 1	-168 ± 5	
LC2 600 + same epochs	-178 ± 3	-187 ± 36	-126 ± 2	-167 ± 8	
LC2 600 + same time span	-200 ± 2	-225 ± 24	-127 ± 2	-177 ± 6	
Division I					-139 ± 68
Division II					-129 ± 53

Note: The GRACE monthly solutions are smoothed using a Gaussian filter with a half-width of 400 km. Furthermore, the estimates are obtained using leakage correction procedure LC2 that refers to the procedure where the mass variations are estimated over the region enlarged with a 600 km buffer. For comparison, the ICESat-based estimates are provided in the last column for two different divisions (I and II) of the Greenland ice sheet, see Section 2.2.
[a]Available for 2003 February to 2006 December.

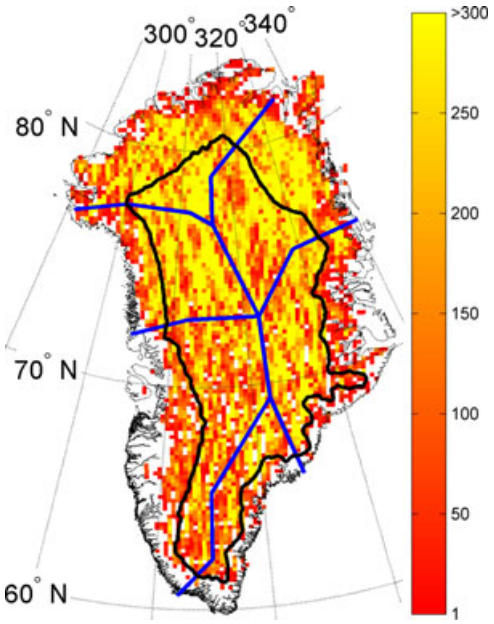

Figure 3. The number of overlapping footprint pairs per grid cell of 20 × 20 km. Empty cells are left blank.

whole Greenland coast, less overlapping footprint pairs are available, which may hamper a representative description of the ablation signals in this region. Additionally, the influence of surface slope, surface roughness, saturation etc. is expected to lower the quality of the observations in the coastal areas.

It is also important to recall that the results based on ICESat data are sensitive to the assumed snow/ice density, as volume changes are converted into mass changes. The densities we used should be considered as a very first guess that virtually does not take into account spatial and temporal variations, which reflect such processes as accumulation of fresh snow, summer melting of surface material with a subsequent migration of the meltwater inside the glacier and its freezing, long-term compaction of surface materials, etc.

Finally, from Table 4 we conclude that the estimated mass change rates based on different sets of monthly solutions show minimal differences for the DEOS solutions, while for the CSR solutions the maximal differences are observed. Especially the differences between the estimates based on the 'ICESat' months (second row Table 4) and 'ICESat' time span (third row Table 4) are striking. For all solutions, stronger mass losses are observed when all months within the same time span are used. This may lead to the conclusion that the use of only two or three laser campaigns of ∼35 d yr^{-1} for ICESat does not provide a representative signal of the real mass change rate for that year. In Fig. 4 we show, using the CNES solutions as an example, that data points in the summer of 2003 and 2004 exceed the estimated trend. This explains why the trend based on the same time span shows a larger ice loss. Therefore, a further analysis of all available data, as well as a collection of new data, is needed to draw more definitive conclusions about the actual rate of ice mass change in Greenland.

5 A JOINT INVERSION OF ICESAT AND GRACE

Both the GRACE- and ICESat-based mass change rates are contaminated by errors from different sources. For ICESat, these were already discussed in the previous section. For GRACE, the presence of errors follows from a relatively large range of estimates obtained on the basis of different GRACE solutions. A joint inversion of both data sets is a way to reduce errors. This is the motivation of the first joint inversion scheme we developed. On the other hand, ICESat data contain physically different information than GRACE data: volume changes instead of mass changes. Therefore, by combining these types of data, one can obtain new knowledge about natural processes in Greenland. This is the idea behind the second joint inversion scheme. Both schemes provide only integrated estimations for the Greenland ice sheet as a whole due to the limited spatial resolution of GRACE data.

5.1 Joint inversion I

5.1.1 Theory

In this section, we present a joint inversion concept that allows to estimate the mass change rate and the parameters of the seasonal cycle (see eq. 2), in combination with the effective snow/ice density, for the whole of Greenland. Basically we have the following system of non-linear observation equations:

$$\begin{cases} \underline{M_i} = M_i + \underline{e}_M \\ \sum \underline{\Delta V}_{ij} = \frac{-M_i + M_j}{\rho} + \underline{e}_{\Delta V}, \quad \text{with } i < j \end{cases} \tag{7}$$

where $\underline{M_i}$ is the mass observed with GRACE at epoch i, M_i the unknown, real mass at epoch i, $\underline{e}_M$ and $\underline{e}_{\Delta V}$ the errors in the observed mass and volume changes, respectively, $\sum \underline{\Delta V}_{ij}$ the volume change observed by ICESat between epoch i and j obtained by summation

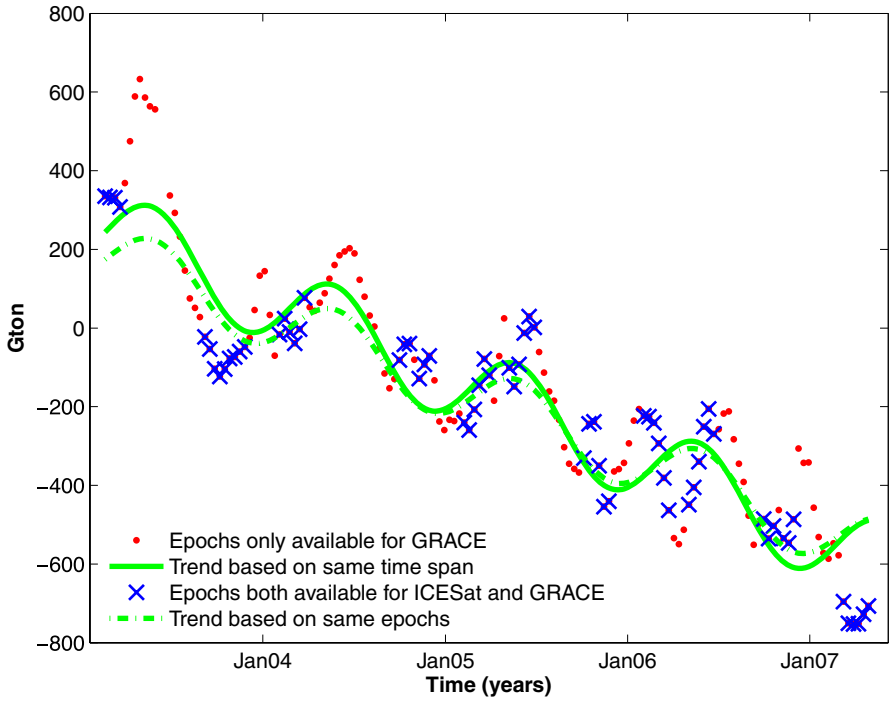

Figure 4. Time-series and estimated trends for CNES solutions using only the months for which ICESat data are available and over the same time span as we have for ICESat data.

over the four regions (see Section 2.2) and ρ the unknown effective snow/ice density. After replacing H_i by M_i in eq. (2), we substitute eq. (2) in eq. (7), so we obtain:

$$\begin{cases} \underline{M}_i = a + \dot{M}t_i + c\sin(ft_i) \\ \qquad\quad +d\cos(ft_i) + \underline{e}_M \\ \sum \Delta\underline{V}_{ij} = \frac{\dot{M}(t_j - t_i) + c\left[\sin(ft_j) - \sin(ft_i)\right]}{\rho} \\ \qquad\quad + \frac{d\cdot\left[\cos(ft_j) - \cos(ft_i)\right]}{\rho} + \underline{e}_{\Delta V}, \quad i < j \end{cases} \tag{8}$$

where $f = 2\pi/T$, with T equal to 1 yr.

To derive the formal error of the total volume change per epoch combination derived from ICESat data, we need to know the variance–covariance matrix $\boldsymbol{Q}_{\Delta H}$ of the observed elevation differences. We assumed that $\boldsymbol{Q}_{\Delta H}$ can be defined as a scaled unit matrix where the scale factor is obtained as the squared standard deviation of the elevation differences for time differences of less than 30 d. It turns out that these standard deviations vary between 0.16 m for drainage system 2a and 1.4 m for drainage system 4b. This can be primarily explained by an increased influence of surface slope and roughness at the coastal regions. With $\boldsymbol{Q}_{\Delta H}$ and the propagation law of variances, we are able to derive the diagonal variance–covariance matrix $\boldsymbol{Q}_{yy\_\mathrm{ICESat}}$ that describes the formal errors of the total volume changes per epoch pair. For GRACE, we derive the diagonal variance–covariance matrix $\boldsymbol{Q}_{yy\_\mathrm{GRACE}}$ of the GRACE mass observations based on the calibrated standard deviations and the propagation law of variances. The combined variance–covariance matrix is obtained with variance component estimation (VCE) that re-estimates the relative weights of the GRACE and ICESat data sets (Teunissen & Amiri-Simkooei 2007). Basically we estimate two scaling factors (σ_1 and σ_2) that are used to scale the variance–covariance matrices of each data set accordingly.

$$\boldsymbol{Q}_{yy_{\mathrm{JI}}} = \sigma_1 \begin{pmatrix} \boldsymbol{Q}_{yy\_\mathrm{GRACE}} & 0 \\ 0 & 0 \end{pmatrix} + \sigma_2 \begin{pmatrix} 0 & 0 \\ 0 & \boldsymbol{Q}_{yy\_\mathrm{ICESat}} \end{pmatrix}. \tag{9}$$

Table 5. Estimated mass change rates in Gton yr^{-1} and the effective snow/ice densities in kg m^{-3}, obtained after a joint inversion of ICESat with each GRACE solution separately and with all GRACE solutions combined.

GRACE solutions	Time span	$\dot{M}$	ρ
CNES	Aug 2002–Jun 2007	-188 ± 8	1213 ± 100
CSR	Apr 2002–Jun 2007	-164 ± 21	1111 ± 160
DEOS	Feb 2003–Dec 2006	-101 ± 9	679 ± 70
GFZ	Aug 2002–Jun 2007	-127 ± 21	875 ± 150
All	Apr 2002–Jun 2007	-175 ± 7	1126 ± 90

Taking this into account, we solve the system of eqs (8) with a non-linear weighted least-squares algorithm.

5.1.2 *Results of joint inversion I*

Table 5 contains the estimated mass change rates and corresponding effective snow/ice densities based on the combination of ICESat with each GRACE solution separately. Additionally we consider the use of all GRACE solutions, which might be reasonable if the differences among the GRACE solutions are interpreted as an evidence of random errors in these solutions.

Looking at the estimated effective densities, we immediately conclude that most of them seem to be physically impossible, because they exceed the density of pure ice, which equals 917 kg m^{-3}. This apparent paradox can be explained by the fact that the nett mass change can be split into a part related to ablation and a part related to accumulation processes for which different densities hold. In the extreme case when the volume change due to ice ablation processes is fully compensated by the accumulation of fresh snow, the nett mass change ΔM is negative while the nett volume change is close to zero. So, the effective density estimated as $\Delta M/\Delta V$ can be a positive or negative value of an arbitrary large magnitude (depending on the sign of ΔV).

Further analysis of the obtained values allows the conclusion to be drawn that spreading of rate estimations is not reduced with respect to stand alone GRACE-based estimations, as one could expect. While the largest negative trend of about $-190\,\mathrm{Gton\,yr^{-1}}$ (CNES solution) is reproduced in both approaches, the smallest trend obtained by the joint inversion ($-101\,\mathrm{Gton\,yr^{-1}}$, DEOS solution) is 20 per cent lower than that derived from GRACE data only. A particularly low trend observed for the DEOS solution can be explained by the fact that the same effective density is now used throughout Greenland to convert volume changes into mass changes. If this effective density is found to be between the actual density of ice and snow (as it is the case for the DEOS solution), the negative mass change in the coastal areas is underestimated because the driving process there is an acceleration of glaciers (Rignot & Kanagaratnam 2006). On the other hand, the positive mass change in the central part of Greenland is overestimated, because a positive volume change there reflects an uncompensated accumulation of snow. In total, the negative mass change rate turns out to be smaller than in reality. Notice further, that there are more reasons why the joint inversion may underestimate actual trends. The exploited ICESat data may lead to an underestimation due to merging drainage systems together (see Section 2.2), whereas the used GRACE models may result in an underestimation due to elimination of the epochs that are not present in ICESat data (see Section 4). In the first case, the underestimation may reach about $10\,\mathrm{Gton\,yr^{-1}}$ (Table 1), while in the second case, the underestimation may reach about $30\,\mathrm{Gton\,yr^{-1}}$ (Table 4).

This analysis allows us to suggest that attempts to combine ICESat and GRACE data, especially using the same effective density in space and time, may lead to not very reliable final estimates. Therefore, we have developed an alternative concept to combine GRACE and ICESat data that aim at a separate estimation of snow and ice volume variations.

5.2 Joint inversion II

5.2.1 Theory

In the alternative joint inversion concept, the combination of ICESat and GRACE data allows the rate of changes in ice volume $\dot{V}^{\mathrm{ice}}$ and snow volume $\dot{V}^{\mathrm{snow}}$ to be estimated separately. This can be done in two ways.

Method A: On basis of the estimation of the volume and mass change rates obtained from ICESat and GRACE data, respectively:

$$\begin{cases} \dot{M} = \dot{V}^{\mathrm{ice}}\rho^{\mathrm{ice}} + \dot{V}^{\mathrm{snow}}\rho^{\mathrm{snow}} + \underline{e}_{\dot{M}} \\ \dot{V} = \dot{V}^{\mathrm{ice}} + \dot{V}^{\mathrm{snow}} + \underline{e}_{\dot{V}} \end{cases}, \tag{10}$$

where $\dot{M}$ and $\dot{V}$ are the estimated mass and volume change rates, respectively, ρ^{ice} and ρ^{snow} the densities of ice and snow, respectively and $\underline{e}_{\dot{M}}$ and $\underline{e}_{\dot{V}}$ the errors in the mass/volume change rates. We defined the density of fresh snow as $\rho^{\mathrm{snow}} = 350\,\mathrm{kg\,m^{-3}}$ and that of ice as $\rho^{\mathrm{ice}} = 900\,\mathrm{kg\,m^{-3}}$. To avoid the effect of a different temporal coverage of ICESat and GRACE data, the same epochs have to be chosen for both sets.

Method B: Alternatively, a time-series of ice and snow volume variations with respect to a fixed reference epoch could be used as input.

To obtain a solvable system of equations, we use a set of derived GRACE observations that describe the mass changes (ΔM_{ij}) between the same pairs of epochs as we have with ICESat. In this case, we can write the system of observation equations for a given pair of epochs as:

$$\begin{cases} \Delta M_{ij} = \Delta V_{ij}^{\mathrm{ice}}\rho^{\mathrm{ice}} + \Delta V_{ij}^{\mathrm{snow}}\rho^{\mathrm{snow}} + \underline{e}_{\Delta M}, \\ \Delta V_{ij} = \Delta V_{ij}^{\mathrm{ice}} + \Delta V_{ij}^{\mathrm{snow}} + \underline{e}_{\Delta V} \end{cases} \tag{11}$$

Notice that when we derive the ΔM_{ij} data vector from the original data vector, also the variance–covariance matrix becomes non-diagonal even if the covariance matrices of monthly solutions are assumed to be diagonal. However, we neglected the off-diagonal elements of this matrix.

This system of linear eqs (11) is solved for all pairs of epochs simultaneously. Again, the combined variance–covariance matrix is obtained with the VCE technique, see Section 5.1. This results in separate snow and ice volume changes between all pairs of epochs available for ICESat. To retrieve a time-series from these changes, we use the same methodology as described in chapter 2, developed to construct the time-series of elevations based on the observed elevation differences with ICESat. These time-series are used consecutively to estimate separate linear trends, jointly with a seasonal cycle, for ice and snow volume, respectively.

5.2.2 Results of joint inversion II

The obtained time-series of snow and ice volume variations as well as their analytical approximations are shown in Figs 5 and 6. It is interesting to see that the time-series that describes the snow volume changes reaches the maximum in April/May (Fig. 5), which corresponds to the end of the accumulation season. The ice volume variation shows a much less prominent seasonal variability. The seasonal maximum is reached in July/August. A possible explanation is a massive melting of snow at the surface with a subsequent freezing of the meltwater inside the ice layer. Thus, the rate of formation of new ice exceeds the rate of ablation due to melting and calving of glaciers. In the winter time, the relationship between ice formation and ablation is opposite. Our interpretation is consistent with the fact that the peak of surface ice melting takes place at the end of July (Abdalati & Steffen 1997).

Table 6 contains the estimated volume change rates for the combination of each GRACE solution with ICESat data separately as well as all together. Here, we obtained the volume change rates both with the use of eq. (10) (method A) and after the estimation of the time-series of ice and snow volume variations (method B). Most combinations show an increasing snow volume and a decreasing ice volume. This is consistent with other studies that showed a growth of the interior of the ice sheet as a consequence of increased accumulation (Johannessen *et al.* 2005). Furthermore, all the solutions show a negative trend in ice volume changes. This is in agreement with an increased mass loss in the coastal regions, due to accelerated glacier flows (Rignot & Kanagaratnam 2006). Note that for all combinations of ICESat with the different GRACE solutions, the use of ice sheet division II, to obtain the total volume changes for ICESat, results in an additional snow volume change rate of $18\,\mathrm{Gton\,yr^{-1}}$ and an additional ice volume loss of $7\,\mathrm{Gton\,yr^{-1}}$, compared to division I. Assuming that these differences reflect a bias caused by an insufficiently representative distribution of footprints, we can apply a corresponding correction to any solution obtained on the basis of division II. For the estimates obtained on the basis of all GRACE models simultaneously (last line in table 6), this results in the following rates: $\dot{V}^{\mathrm{snow}} = 92 \pm 14\,\mathrm{km^3\,yr^{-1}}$; $\dot{V}^{\mathrm{ice}} = -235 \pm 8\,\mathrm{km^3\,yr^{-1}}$.

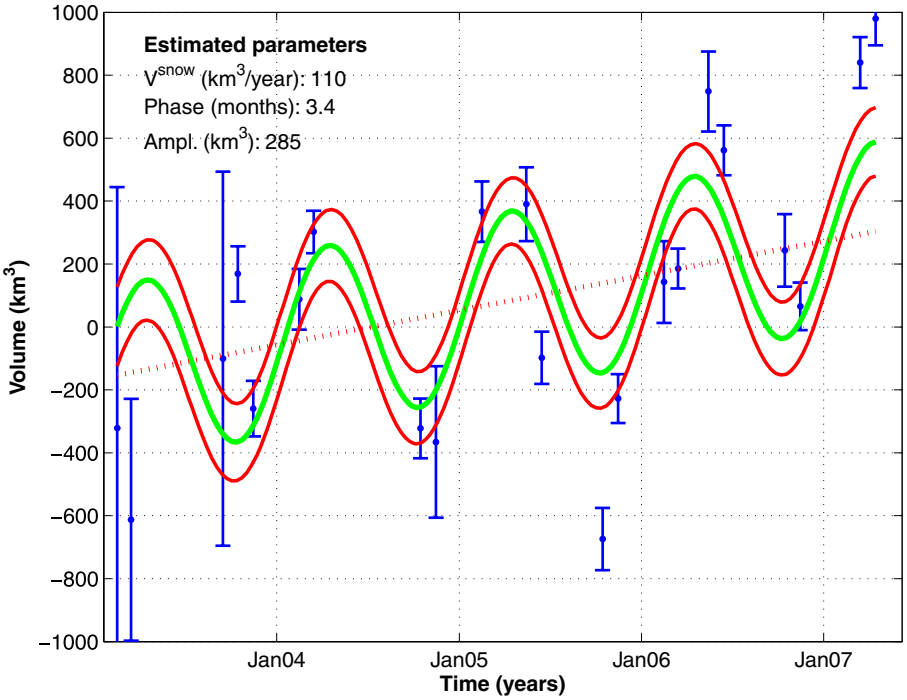

Figure 5. Estimated time-series as well as their analytical approximation of snow volume changes based on a joint inversion of ICESat data and all GRACE solutions (method B). The estimated trend is represented as the straight dotted line, while the solid green line is the trend plus the seasonal cycle. The solid red curves represent the 95 per cent confidence interval.

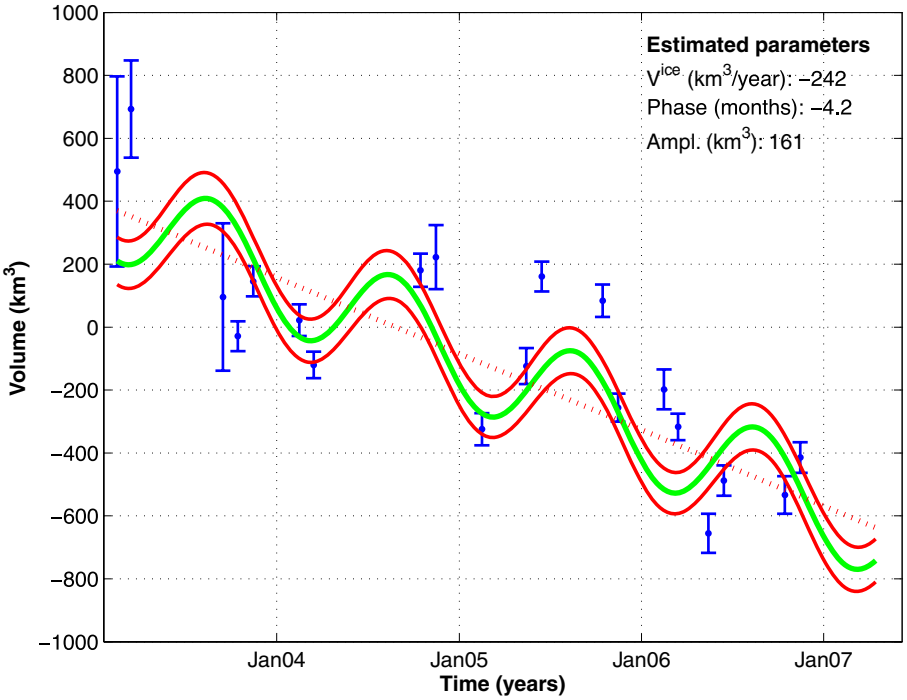

Figure 6. Estimated time-series as well as their analytical approximation of ice volume changes based on a joint inversion of ICESat data and all GRACE solutions (method B). The estimated trend is represented as the straight dotted line, while the solid green line is the trend plus the seasonal cycle. The solid red curves represent the 95 per cent confidence interval.

6 CONCLUSIONS

Based on ICESat data alone, the most probable estimation of the average Greenland mass change rate between 2003 February and 2007 April is -139 ± 68 Gton yr^{-1}, which can be mainly attributed to strong mass losses in the region below 2000 m (-151 ± 52 Gton yr^{-1}). Based on GRACE data alone, we conclude that the estimated mass change rate is in the range between -128 and -218 Gton yr^{-1}. The time span of most GRACE solutions is, however, wider (middle 2002–middle 2007). Furthermore, GRACE

Table 6. Estimated snow and ice volume change rates over a time span of 2003 February to 2007 April in $km^3\ yr^{-1}$, using eq. (10) (method I) and after the estimation of the trend from the estimated time-series (method II).

GRACE solutions	Division	Method A $\dot{V}^{snow}$	Method A $\dot{V}^{ice}$	Method B $\dot{V}^{snow}$	Method B $\dot{V}^{ice}$
CNES	I	83 ± 5	-230 ± 5		
	II	101 ± 5	-237 ± 5	140 ± 37	-271 ± 27
CSR	I	99 ± 66	-246 ± 66		
	II	117 ± 66	-253 ± 66	173 ± 77	-299 ± 50
DEOS	I	-11 ± 5	-136 ± 4		
	II	6 ± 4	-143 ± 4	37 ± 22	-155 ± 22
GFZ	I	63 ± 15	-210 ± 15		
	II	81 ± 15	-217 ± 15	55 ± 63	-213 ± 44
All	II			110 ± 14	-242 ± 8

solutions contain much less temporal gaps than the ICESat solution. Selection of GRACE solutions only on the months when ICESat data are available reduces the range of estimated trends to between -126 and -187 Gton yr^{-1}.

A joint inversion of ICESat and GRACE data into a series of mass variations has not reduced the range of uncertainties, and, therefore, cannot be considered as successful. A probable reason is the fact that the effective density needed to convert ICESat data into mass change is assumed to be constant in space and time. This assumption might not be realistic because the observed volume changes are associated with two materials of totally different densities: ice and snow. The second concept of joint inversion, where ice and snow volume changes are estimated separately, seems to be reasonable. Based on this concept, we obtained for different GRACE solutions a snow volume change rate in the range of -11 to $155\ km^3\ yr^{-1}$ and an increasing ice loss with a rate between -136 and $-292\ km^3\ yr^{-1}$. The most probable estimates obtained on the basis of all GRACE models simultaneously are: $\dot{V}^{snow} = 92 \pm 14\ km^3\ yr^{-1}$; $\dot{V}^{ice} = -235 \pm 8\ km^3\ yr^{-1}$.

Note, that for both joint inversion schemes, systematic errors for ICESat data [e.g. undersampling problem (Section 4)] are not taken into account, which is considered as a topic for future work. Furthermore, the influence of snow compaction (Section 2.3) should be removed before application of the joint inversion schemes. Here, existing models could be used (Li *et al.* 2007a). Also in future research, more accurate data processing strategies to obtain the GRACE models should be developed to reduce the spread between different GRACE solutions.

So far, we produced only integrated estimations of ice and snow volume changes for the whole of Greenland. However, the same concept can also be applied to different drainage systems separately, which will provide more insight into the mass accumulation and ablation processes in Greenland. To that end, state-of-the-art high resolution models of mass variations in Greenland have to be exploited.

ACKNOWLEDGMENTS

We would like to thank R.E.M. Riva for the computation of the PGR corrections and X.L. Liu, who provided us with the DEOS global gravity field models. Furthermore, we are grateful to E.A. Revtova for the software to process gravity field models. Also we would like to thank J. Wahr and one anonymous reviewer for their useful comments on earlier versions of this manuscript.

REFERENCES

Abdalati, W. & Steffen, K., 1997. Snowmelt on the Greenland ice sheet as derived from passive microwave satellite data, *J. Clim.,* **10,** 165–175.

Arthern, R.J. & Wingham, D.J., 1998. The natural fluctuations of firn densification and their effect on the geodetic determination of ice sheet mass balance, *Clim. Change,* **40**(3–4), 605–624.

Bettadpur, S., 2007. *CSR Level-2 Processing Standards Document For Product Release 04, GRACE* 327-742, Center for Space Research, University of Texas at Austin.

Chen, J.L., Wilson, C.R. & Tapley, B.D., 2006. Satellite gravity measurements confirm accelerated melting of Greenland ice sheet, *Science,* **313,** 1958–1960.

DiMarzio, J., Brenner, A., Schutz, R., Shuman, C.A. & Zwally, H.J., 2007. *GLAS/ICESat 1 km Laser Altimetry Digital Elevation Model of Greenland,* Digital media, National Snow and Ice Data Center, Boulder, CO.

Howat, I.M., Joughin, I. & Scambos, T.A., 2007. Rapid changes in ice discharge from Greenland outlet glaciers, *Science,* **315**(5818), 1559–1561.

IPCC, 2007. Climate Change 2007: Synthesis Report, Summary for Policymakers, available at: http://www.ipcc.ch/pdf/assessment-report/ar4/syr/ar4_syr_spm.pdf, accessed February, 2008.

Johannessen, O.M., Khvorostovsky, K., Miles, M.W. & Bobylev, L.P., 2005. Recent ice-sheet growth in the interior of Greenland, *Science,* **310,** 1013–1016.

Klees, R., Zapreeva, E.A., Winsemius, H.C. & Savenije, H.H.G., 2007. The bias in GRACE estimates of continental water storage variations, *Hydrol. Earth Sys. Sci.,* **11,** 1227–1241.

Lemoine, J.M., Bruinsma, S., Loyer, S., Biancale, R., Marty, J.C., Perosanz, F. & Balmino, G., 2007. Temporal gravity field models inferred from GRACE data, *Advances is Space Research*, **39,** 1620–1629.

Li, J., Zwally, H.J. & Comiso, J.C., 2007a. Ice-sheet elevation changes caused by variations of the firn compaction rate induced by satellite-observed temperature variations (1982-2003), *Ann. Glaciol.,* **46**(6), 8–13.

Li, J., Zwally, H.J. & Comiso, J.C., 2007b. Increased rates of surface elevation change driven by the surface temperature (1982-2006) over the Greenland Ice Sheet, *Abstracts AGU Fall Meeting,* A80+.

Liu, X., Ditmar, P., Zhao, Q., 2007. A new variant of the acceleration approach for gravity field modelling from GRACE range measurements. Poster presentation at the General Assembly of the European Geosciences Union, Viena, Austria, 15–20 April 2007.

Luthcke, S.B. *et al*., 2006. Recent Greenland ice mass loss by drainage system from satellite gravity observations, *Science,* **314,** 1286–1289.

Peltier, W.R., 2004. Global glacial isostasy and the surface of the ice-age Earth: the ICE-5G (VM2) Model and GRACE, *Ann. Rev. Earth Planet. Sci.,* **32,** 111–149.

Ramillien, G., Lombard, A., Cazenave, A., Ivins, E.R., Llubes, M., Remy, F. & Biancale, R., 2006. Interannual variations of the mass balance of

the Antarctica and Greenland ice sheets from GRACE, *Global Planet. Change,* **53,** 198–208.

Rignot, E.J. & Kanagaratnam, P., 2006. Changes in the velocity structure of the Greenland ice sheet, *Science,* **311,** 986–990.

Schmidt, R., 2007. *Static field Geopotential Coefficients Estimated from Satellite Data Only,* Digital media., GFZ Potsdam GRACE Science Data System, Oberpfaffenhofen, Germany.

Slobbe, D.C., Lindenbergh, R.C. & Ditmar, P., 2008. Estimation of volume change rates of Greenland's ice sheet from ICESat data using overlapping footprints, *Remote Sensing Environ.,* in press.

Swenson, S. & Wahr, J., 2006. Post-processing removal of correlated errors in GRACE data, *Geophys. Res. Lett.,* **33,** L08402.

Teunissen, P.J.G. & Amiri-Simkooei, A.R., 2007. Least-squares variance component estimation, *J. Geod.,* **82,** 65–82.

Thomas, R., Frederick, E., Krabill, W., Manizade, S. & Martin, C., 2006. Progressive increase in ice loss from Greenland, *Geophys. Res. Lett.,* **33,** L10503.

Velicogna, I. & Wahr, J., 2005. Greenland mass balance from GRACE, *Geophys. Res. Lett.,* **32,** L18505.

Velicogna, I. & Wahr, J., 2006. Acceleration of Greenland ice mass loss in spring 2004, *Nature,* **443,** 329–331.

Velicogna, I. & Wahr, J., 2007. Seasonal and long term ice mass variations from GRACE, in *Proceedings of IUGG XXIV 2007, Earth: Our Changing Planet*, International Association of Geodesy.

Wahr, J., Molenaar, M. & Bryan, F., 1998. Time variability of the Earth's gravity field: hydrological and oceanic effects and their possible detection using GRACE, *J. geophys. Res.,* **103,** 30 205–30 230.

Wahr, J., Wingham, D. & Bentley, C., 2000. A method of combining ICESat and GRACE satellite data to constrain Antarctic mass balance, *J. geophys. Res.,* **105,** 16 279–16 294.

Wahr, J., Swenson, S. & Velicogna, I., 2007. Some hydrological and cryospheric applications of GRACE, in *Proceddings of GSTM + DFG-SPP Symposium in Potsdam,* accessed February, 2008.

Wingham, D.J., Shepherd, A., Muir, A. & Marshall, G.J., 2006. Mass balance of the Antarctic ice sheet, *R. Soc. Lond. Philos. Trans. Series A,* **364,** 1627–1635.

Zwally, H.J., Giovinetto, M.B., Li, J., Cornejo, H.G., Beckley, M.A., Brenner, A.C., Saba, J.L. & Yi, D., 2005. Mass changes of the Greenland and Antarctic ice sheets and shelves and contributions to sea-level rise: 1992-2002, *J. Glaciol.* **51,** 509–527.

Zwally, H.J., Schutz, R., Bentley, C., Bufton, J., Herring, T., Minster, B., Spinhirne, J. & Thomas, R., 2007. *GLAS/ICESat L2 Antarctic and Greenland Ice Sheet Altimetry Data* V001., Digital media, National Snow and Ice Data Center, Boulder, CO.